chemistry proceedings

MDPI

Proceeding Paper

The Influence of High Temperature on X-Ray Luminescence Performance of BGO and BaF_2 Scintillation Crystals †

Theodoros Tryfonidis, Dionysios Linardatos, Vasileios Ntoupis, George Saatsakis, Ioannis Valais, Nektarios Kalyvas, George Fountos, Ioannis Kandarakis and Christos Michail *

Department of Biomedical Engineering, Radiation Physics, Materials Technology and Biomedical Imaging Laboratory, University of West Attica, 12210 Athens, Greece; bme20388096@uniwa.gr (T.T.); dlinardatos@uniwa.gr (D.L.); vdoupis@uniwa.gr (V.N.); gsaatsakis@uniwa.gr (G.S.); valais@uniwa.gr (I.V.); nkalyvas@uniwa.gr (N.K.); gfoun@uniwa.gr (G.F.); kandarakis@uniwa.gr (I.K.)

* Correspondence: cmichail@uniwa.gr

† Presented at the 5th International Online Conference on Crystals, 15–17 June 2026; Available online: https://sciforum.net/event/IOCC2026.

Abstract

This study examines the luminescence performance of two single-crystal scintillators under X-ray excitation, as a function of temperature. Two identical cubic samples of bismuth germanate ($Bi_4Ge_3O_{12}$-BGO) and barium fluoride (BaF_2) crystals are irradiated by a medical-type X-ray source, and their luminescence output is collected and measured while they are heated from room temperature up to 174 °C. The luminescence efficiencies of BGO and BaF_2 scintillators decreased by 87.5% and 79.48%, respectively, with increasing temperature. BGO showed higher luminescence efficiency results in most of the examined temperature range; however, BaF_2 minimized the differences at temperatures approaching 174 °C. The combination of economic accessibility and thermal performance at higher temperatures renders BaF_2 a good choice for harsh environments and large-scale applications where budget and durability are as critical as performance.

Keywords: single crystals; BGO; BaF_2; thermal behavior; extreme environments; medical imaging

1. Introduction

Crystal scintillators are widely used in imaging applications, including medical settings, and some of them require the crystal to operate at higher temperatures [1–3]. Bismuth germanate ($Bi_4Ge_3O_{12}$-BGO) is a well-known single-crystal scintillator, finding applications in numerus imaging modalities, such as positron emission tomography (PET), or even in extreme environments [4,5]. BGO has light yield (LY) ranging between 8.2 and 8.9 $\times$ 10^3 photons/MeV [6]. Furthermore, it has a decay time equal to 300 ns [6] and a 2.5 $\times$ 10^3 to 6 $\times$ 10^3 ps @ FWHM timing resolution [7]. An indicative market price for a 10 $\times$ 10 $\times$ 1 mm^3 BGO crystal is about 188.95 USD [8]. However, BGO has some limitations regarding its application in high-energy physics, such as the difficulty of large-scale crystal production, as well as the afterglow emerging from radiation damage [5].

Barium fluoride (BaF_2) is an inorganic scintillator the combines balanced luminescence performance (light yield of 1 $\times$ 10^4 photons/MeV (slow component); 1.8 $\times$ 10^3 photons/MeV (fast component); and 1.18 $\times$ 10^4 photons/MeV (total) [9,10]; rapid temporal resolution [11,12]; and fast decay (around 0.6–0.87 ns) [13,14]. Because of these it is ideal for application in

Check for updates

Academic Editor: Stanislav Ferdov

Published: 28 August 2026

Copyright: © 2026 by the authors. Licensee MDPI, Basel, Switzerland. This article is an open access article distributed under the terms and conditions of the Creative Commons Attribution (CC BY) license.

medical detectors, such as time-of-flight (ToF) PET and ToF computed tomography (TOF-CT) systems [14,15].

Furthermore, BaF_2 has a decent radiation hardness (10^6–10^7 [16]), has good chemical stability, and is non-hygroscopic [7]), properties that render it suitable for harsh environments [17,18] and high-energy physics applications [19,20]. Barium fluoride has also been proposed for applications in nuclear research, near- and mid-infrared optical coherence tomography (OCT), non-destructive testing (NDT), infrared thermographic monitoring [21,22] and dose monitoring in radiation therapy [11,23,24].

BaF_2 appears as a cheaper alternative to more expensive materials like BGO, whereas a BaF_2 single crystal with similar dimensions ($10 \times 10 \times 1$ mm^3) costs about 83.95 USD [25].

While the response of BGO crystals under excitation with alpha particles and gamma rays has been previously reported to fall with increasing temperature [26–29], there is a distinct lack of comparative literature regarding their continuous performance under medical X-ray spectra at elevated temperatures reaching 174 °C.

Since BaF_2 has a much lower cost than BGO, in this work, the luminescence efficiency of BGO and BaF_2 inorganic scintillators is examined under X-ray irradiation for possible application in imaging modalities operating at temperatures different from the environment.

2. Materials and Methods

2.1. Experimental Setup

Both the examined crystal samples had dimensions of $1 \times 1 \times 1$ cm and polished surfaces. Irradiation was performed using a DR 200 CMP CPI X-ray medical system (CPI Inc., Camarillo, CA, USA). The irradiation parameters were set to 90 kVp, 63 mA, and 1 s, with the 0.12 cm focus on. The distance from the X-ray focus to crystal's surface was set to 0.725 m. An additional 2 cm aluminum (Al) filter was placed on the X-ray tube output [10].

The crystal samples were placed on the input window of an integration sphere (Newport Corp., Irvine, CA, USA, model Oriel 70451) and the luminescence generated upon X-ray excitation was detected using a photomultiplier tube (PMT, EMI, London, UK, model 9798) attached to another window of the integrating sphere. The PMT (EMI 9798) employed an extended-sensitivity (S20) photocathode. In addition, the PMT operated with a voltage of 22 V applied to the photocathode and the first dynode. Dynodes were short-circuited. Dose was measured with a Piranha digital dosimeter (RTI, Mölndal, Sweden, model Piranha P100B).

Heating of the crystal samples was performed using a heating gun (Bulle PLD2372, Bulle, Athens, Greece). Their temperature was controlled by a thermocouple probe (U1185A, Keysight Technologies, Santa Rosa, CA, USA) fixed on the sample's surface using Teflon tape. Attention was paid to leaving one face of the crystal cube uncovered, to allow the light produced from the crystal mass to reflect on the inner surface of the integrating sphere. The temperature on the crystal surface was monitored with a digital multimeter (Agilent Technologies U1253A, Agilent Technologies, Santa Rosa, CA, USA) and a thermocouple. The temperature range was between 19 °C and 174 °C.

2.2. Luminescence Efficiency

The luminescence efficiency of the examined BGO and BaF_2 crystals was estimated through the measurement of X-ray exposure and the produced light energy flux. The light flux, normalized by the X-ray exposure, is given by Equation (1):

$$AE = \eta_A = \frac{\dot{\Psi}_\lambda}{\dot{X}} \quad (1)$$

https://doi.org/10.3390/chemproc2026021004

$\dot{\Psi}_\lambda$ represents the light energy flux (units $\mu W/m^2$) and $\dot{X}$ represents the exposure rate (units mR/s). The AE units are $(\mu W/m^2)/(mR/s)$, with the efficiency units denoted as EU.

The output signal or light energy flux is given by [30]:

$$\dot{\Psi}_\lambda = \frac{i_{elec}}{S \cdot \eta_p \cdot \alpha_s \cdot c_g} \quad (2)$$

where i_{elec} is the PMT current, as measured by the electrometer, in pA. S is the irradiated area of the scintillator, in mm^2. n_p is the photocathode's peak photosensitivity, in $pA \cdot W^{-1}$. α_s is the spectral matching factor (SMF) between the crystal's emitted spectrum and the photocathode's spectral response. c_g is the geometric light collection efficiency of the experimental setup, including the integrating sphere, estimated as 15.6 for our specific geometry.

3. Results and Discussion

Figure 1 shows the emission spectra of BGO and BaF_2 crystals, along with the spectral sensitivity of the photocathode (S20 with extended sensitivity) that was used in the experiments to capture the produced light from the examined samples. The luminescence spectra of these crystals differ considerably, with BGO having an emission maximum at around 490 nm, and BaF_2 at 310 nm. The luminescence maximum values result in different spectral matching with the S20 photocathode (SMF = 0.78 and 0.73 for BGO and BaF_2, respectively). In order to maintain identical irradiation conditions, and to eliminate excitation variables, the spectral mismatch of the two samples was resolved at the detection stage by applying a rigorous correction factor (α_s in Equation (2)) based on the photocathode's spectral response.

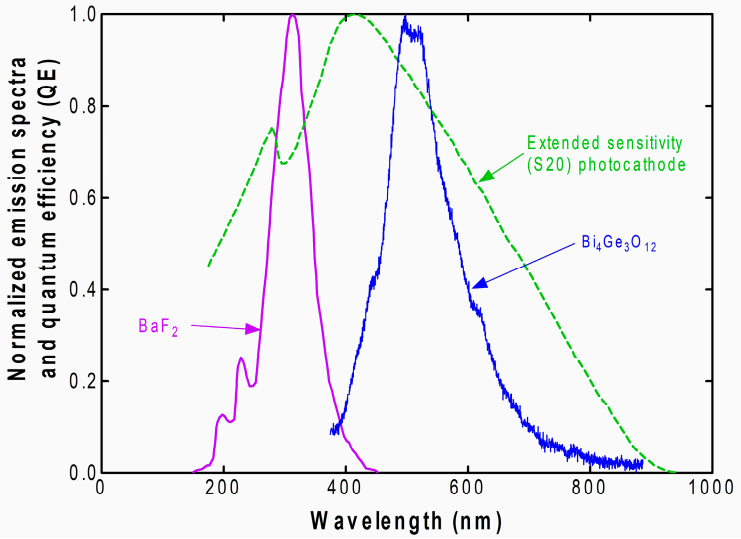


Figure 1. Emission spectra of BGO (blue curve) and BaF_2 (purple curve) crystals, along with the spectral sensitivity of the extended-sensitivity (S20) photocathode (green curve).

Figures 2 and 3 show indicative digitized voltage readings as a function of time for various temperatures of the BGO and BaF_2 crystals, respectively. The readings were obtained through an analog-to-digital converter (ADC) connected to the electrometer output. The ADC input was maintained below 1 V by selecting the appropriate electrometer voltage range according to the intensity of the generated scintillation light. This 1 V range was selected to maximize the available digitization resolution. The electrometer provides selectable voltage ranges from 100 mV to 30 V. Thus, as the generated light signal increased, a higher electrometer range was selected to prevent the digitized ADC signal from exceeding 1 V while maintaining the highest practical ADC resolution. For

the measurements presented here, the selected electrometer ranges were 1 V for BGO and 300 mV for BaF_2. The selected electrometer range was considered in the conversion of the measured signal to the PMT current and in the subsequent calculation of the absolute luminescence efficiency.

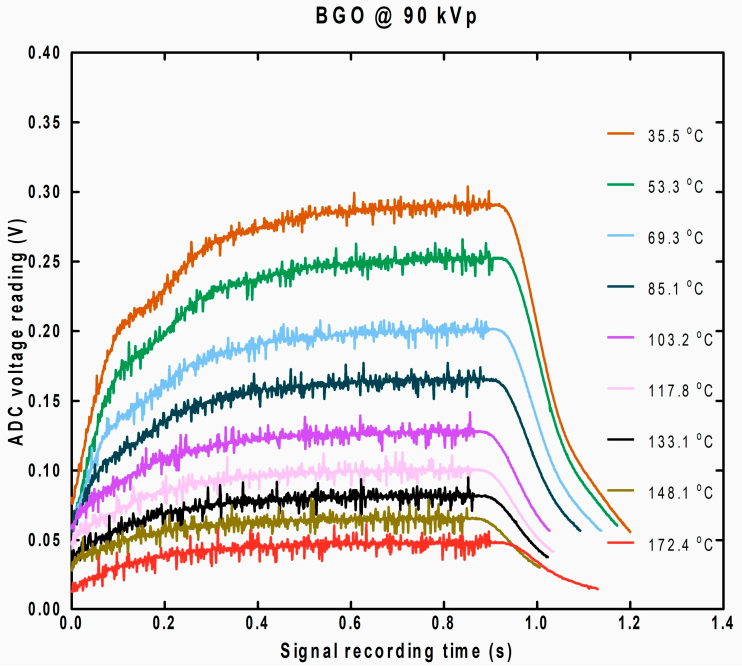


Figure 2. ADC voltage readings of the BGO crystal as a function of time for various temperatures. Fixed exposure of 1 s and electrometer voltage scale of 1 V.

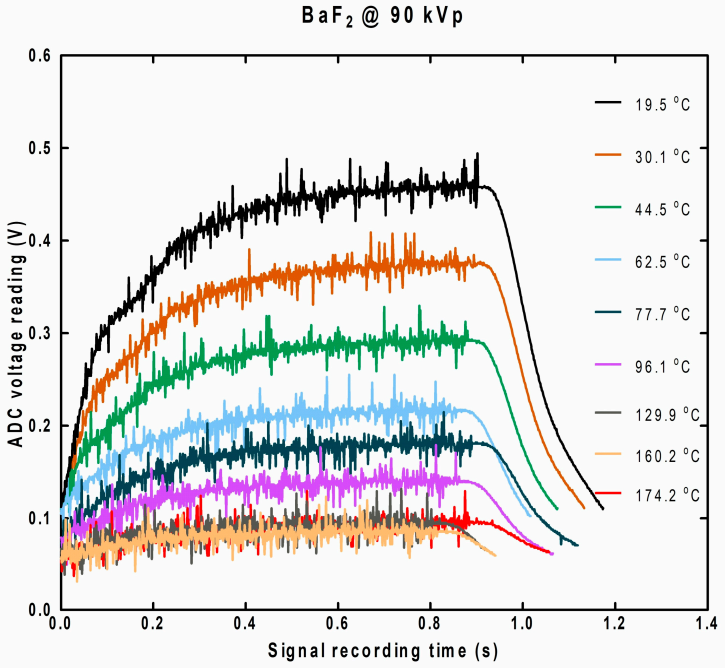


Figure 3. ADC voltage readings of the BaF_2 crystal as a function of time for various temperatures. Fixed exposure of 1 s and electrometer voltage scale of 300 mV.

The time–voltage curves were produced by recording the signal emerging from our measuring instrumentation and by subtracting the time period elapsed to build up the X-ray photon fluence (X-ray beam intensity) of the nominal combination of kVp-mAs.

https://doi.org/10.3390/chemproc2026021004

Furthermore, with increasing temperature the maximum signal diminishes for both scintillators, albeit with different rates. The BGO ADC voltage values peaked at 0.35 V with the electrometer voltage scale set at 1 V. The BaF_2 plateau ADC voltage values were in the range of 0.13 to 0.49 V, with the electrometer voltage scale set at 300 mV.

The ratio of light flux to X-ray exposure for the examined crystals is shown in Figure 4 for various temperatures above environmental. The produced signals of both BGO and BaF_2 crystals drop with temperature, following a similar pattern. This reduction in the luminescence signal (thermal quenching) with temperature relates to the non-radiative relaxation processes within the scintillator crystal that enhance with increasing temperature [31]. The luminescence efficiency for BGO decreases with increasing temperature, ranging from 2.96 EU to 0.37 EU in the temperature range 21.0 °C to 172.4 °C. Similarly, BaF_2 AE ranges from 1.56 EU to 0.32 EU in the range 19.5 °C to 174.2 °C. The luminescence efficiencies of BGO and BaF_2 crystals decrease with increasing temperature by 87.51% and 79.48%, respectively. Similar behavior is reported in the literature [27,32,33]. At 172.4 °C BGO drops down to 0.37 EU, whereas the corresponding value for BaF_2 is 0.32 EU at 174 °C, despite their luminescence differences at room temperature.

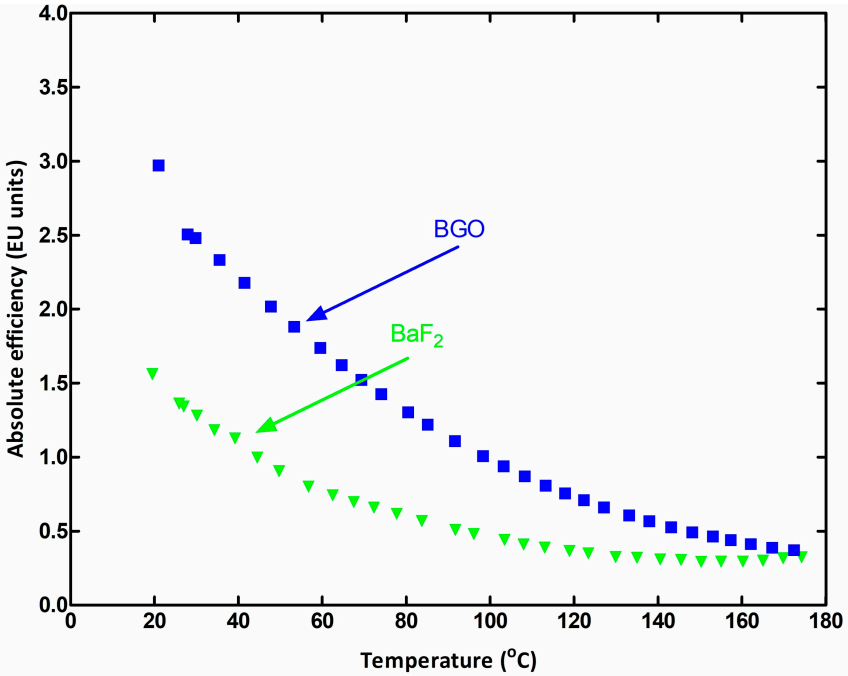


Figure 4. Comparative luminescence performance of BGO (blue squares) and BaF_2 (green triangles) samples in the examined temperature range of 19–174 °C.

4. Conclusions

This study examines the X-ray luminescence performance of BGO and BaF_2 single-crystal scintillators under different temperatures. Despite the fact that BGO appeared to exhibit higher LE, in most of the examined temperature range, BaF_2 reduction in the luminescence signal was less apparent, with AE values significantly closer to that of BGO at the higher examined temperatures (174 °C), despite their initial differences.

Consequently, BaF_2 might serve as a highly cost-effective alternative to BGO for high-temperature conditions, offering a compelling solution for radiation detection applications. This combination of economic accessibility and thermal stability at high temperatures renders it a promising scintillator for harsh environments and large-scale applications where budget and durability are as critical as performance.

Author Contributions: Conceptualization, C.M., I.V. and T.T.; methodology, C.M., T.T., V.N., I.V., D.L., N.K., G.F. and I.K.; software, T.T., I.V., V.N. and D.L.; validation, N.K. and I.K.; formal analysis, C.M., N.K., T.T., G.S. and V.N.; investigation, C.M., T.T., N.K., G.F., V.N., D.L. and I.V.; resources, G.F.; data curation, C.M., T.T., N.K., V.N., G.S., G.F. and I.K.; writing—original draft preparation, C.M.; writing—review and editing, C.M., T.T., I.K., N.K., G.S., D.L. and I.V.; visualization, I.V.; supervision, C.M.; project administration, C.M. and I.V. All authors have read and agreed to the published version of the manuscript.

Funding: This research received no external funding.

Institutional Review Board Statement: Not applicable.

Informed Consent Statement: Not applicable.

Data Availability Statement: The data are contained within this article.

Conflicts of Interest: The authors declare no conflicts of interest.

References

1. Li, K.; Li, W.; Nie, Q.; Luo, X. Innovations in Scintillator Materials for X-Ray Detection. *Inorg. Chem. Front.* **2025**, *12*, 4741–4768. [CrossRef]
2. Michail, C.; Liaparinos, P.; Kalyvas, N.; Kandarakis, I.; Fountos, G.; Valais, I. Phosphors and Scintillators in Biomedical Imaging. *Crystals* **2024**, *14*, 169. [CrossRef]
3. Zang, Z.; Xiong, Y.; Zheng, Y.; Qaid, S.M.H.; Cai, W.; Wang, B. Hot-Pressing of Single Crystals Enables High-Performance White-Light Emitting Copper Halide Scintillators Toward Underwater X-Ray Imaging. *Laser Photonics Rev.* **2026**, e71348. [CrossRef]
4. Yu, Z.; Asch, H.; Gerber, R.; Redey, A.; Starosta, K.; Tam, D.; Woinoski, A. Novel Application of the 8π Gamma-Ray Spectrometer for 3γ Positron Emission Tomography. *Nucl. Instrum. Methods Phys. Res. A* **2026**, *1084*, 171168. [CrossRef]
5. Deng, Y.; Xu, Y.; Qian, C.; Wei, D.; Peng, G.; Xie, H.; Wang, H.; Li, Q.; Ci, Z.; Wang, Q.; et al. Manganese Halide-Based Glass-Ceramic Scintillator for Ultra-Stable and Multi-Functional X-Ray Imaging in Extreme Environments. *Laser Photonics Rev.* **2025**, *19*, e01178. [CrossRef]
6. Lecoq, P. Development of New Scintillators for Medical Applications. *Nucl. Instrum. Methods Phys. Res. A* **2016**, *809*, 130–139. [CrossRef]
7. Anderson, D.F. Properties of the High-Density Scintillator Cerium Fluoride. *IEEE Trans. Nucl. Sci.* **1989**, *36*, 137–140. [CrossRef]
8. MSE Supplies LLC. BGO—Bismuth Germanate $Bi_4Ge_3O_{12}$ Scintillation Crystal. Available online: https://www.msesupplies.com/products/bgo-bismuth-germanate-bi4ge3o12-scintillation-crystal (accessed on 28 January 2025).
9. Moses, W.W. Recent Advances and Future Advances in Time-of-Flight PET. *Nucl. Instrum. Methods Phys. Res. A* **2007**, *580*, 919–924. [CrossRef] [PubMed]
10. Ntoupis, V.; Michail, C.; Kalyvas, N.; Bakas, A.; Kandarakis, I.; Fountos, G.; Valais, I. Light Output Response of a Barium Fluoride (BaF_2) Inorganic Scintillator Under X-Ray Radiation. *Inorganics* **2025**, *13*, 83. [CrossRef]
11. Gundacker, S.; Pots, R.H.; Nepomnyashchikh, A.; Radzhabov, E.; Shendrik, R.; Omelkov, S.; Kirm, M.; Acerbi, F.; Capasso, M.; Paternoster, G.; et al. Vacuum Ultraviolet Silicon Photomultipliers Applied to BaF_2 Cross-Luminescence Detection for High-Rate Ultrafast Timing Applications. *Phys. Med. Biol.* **2021**, *66*, 114002. [CrossRef] [PubMed]
12. Seliverstov, D.M.; Demidenko, A.A.; Garibin, E.A.; Gain, S.D.; Gusev, Y.I.; Fedorov, P.P.; Kosyanenko, S.V.; Mironov, I.A.; Osiko, V.V.; Rodnyi, P.A.; et al. New Fast Scintillators on the Base of BaF_2 Crystals with Increased Light Yield of 0.9 Ns Luminescence for TOF PET. *Nucl. Instrum. Methods Phys. Res. A* **2012**, *695*, 369–372. [CrossRef]
13. Advatech UK. BaF_2—Barium Fluoride Scintillator Crystal. Available online: https://www.advatech-uk.co.uk/baf2.html (accessed on 19 December 2024).
14. Herweg, K.; Nadig, V.; Schulz, V.; Gundacker, S. On the Prospects of BaF_2 as a Fast Scintillator for Time-of-Flight Positron Emission Tomography Systems. *IEEE Trans. Radiat. Plasma Med. Sci.* **2023**, *7*, 241–252. [CrossRef]
15. Shendrik, R.; Radzhabov, E.; Myasnikova, A.; Pankratova, V.; Šarakovskis, A.; Nepomnyashchikh, A.; Bogdanov, A.; Gavrilenko, V.; Kaneva, E.; Sofich, D.; et al. Ultrafast Core-to-Core Luminescence in BaF_2-LaF_3 Single Crystals. *Sci. Rep.* **2025**, *15*, 26558. [CrossRef] [PubMed]
16. Kobayashi, M.; Ishii, M. Effect of Cerium Doping on the Radiation Hardness of Gadolinium Silicate Gd_2SiO_5. *Nucl. Instrum. Methods Phys. Res. B* **1993**, *82*, 85–90. [CrossRef]
17. Meenal; Aghwariya, M.K.; Goel, T.; Patnaik, A. Advanced Materials for RF Sensors in Harsh Environments: A Comprehensive Review. *IEEE Sens. Rev.* **2025**, *2*, 324–338. [CrossRef]

18. Sahu, S.K.; Mazumdar, K.; Kumar, S. A Systematic Analysis on the Applications of AlGaN/GaN HEMT for High-Performance Sensing. *IEEE Sens. Rev.* **2025**, *2*, 479–497. [CrossRef]
19. Andrade, A.B.; Ferreira, N.S.; Valerio, M.E.G. Particle Size Effects on Structural and Optical Properties of BaF_2 Nanoparticles. *RSC Adv.* **2017**, *7*, 26839–26848. [CrossRef]
20. Hu, C.; Zhang, L.; Zhu, R.-Y.; Chen, A.; Wang, Z.; Ying, L.; Yu, Z. BaF_2:Y and ZnO:Ga Crystal Scintillators for GHz Hard X-Ray Imaging. *Nucl. Instrum. Methods Phys. Res. A* **2020**, *950*, 162767. [CrossRef]
21. Turk, T.; Liu, T.; Hung, C.-H.; Billo, R.; Park, J.; Leu, M.C. In-Situ Thermographic Monitoring and Numerical Simulations of Laser-Foil-Printing Additive Manufacturing. *Virtual Phys. Prototyp.* **2025**, *20*, e2440609. [CrossRef]
22. Petersen, C.R.; Rajagopalan, N.; Markos, C.; Israelsen, N.M.; Rodrigo, P.J.; Woyessa, G.; Tidemand-Lichtenberg, P.; Pedersen, C.; Weinell, C.E.; Kiil, S.; et al. Non-Destructive Subsurface Inspection of Marine and Protective Coatings Using Near- and Mid-Infrared Optical Coherence Tomography. *Coatings* **2021**, *11*, 877. [CrossRef]
23. McGregor, D.; Shultis, J.K. *Radiation Detection: Concepts, Methods, and Devices*; CRC Press: Boca Raton, FL, USA, 2020.
24. Kandemir, M.; Tiras, E.; Kirezli, B.; Koca, İ. SSLG4: A Novel Scintillator Simulation Library for Geant4. *Comput. Phys. Commun.* **2025**, *306*, 109385. [CrossRef]
25. MSE Supplies LLC. BaF_2—Barium Fluoride Crystal and Substrates. Available online: https://www.msesupplies.com/products/mse-pro-barium-fluoride-baf-sub-2-sub-crystal-and-substrates (accessed on 28 January 2025).
26. Wang, P.; Zhang, Y.; Xu, Z.; Wang, X. Study on the Temperature Dependence of BGO Light Yield. *Sci. China Phys. Mech. Astron.* **2014**, *57*, 1898–1901. [CrossRef]
27. Gironnet, J.; Mikhailik, V.B.; Kraus, H.; de Marcillac, P.; Coron, N. Scintillation Studies of $Bi_4Ge_3O_{12}$ (BGO) down to a Temperature of 6 K. *Nucl. Instrum. Meth. Phys. Res. A* **2008**, *594*, 358–361. [CrossRef]
28. Nanal, V.; Back, B.B.; Hofman, D.J. Temperature Dependence of BaF_2 Scintillation. *Nucl. Instrum. Methods Phys. Res. A* **1997**, *389*, 430–436. [CrossRef]
29. Schotanus, P.; van Eijk, C.W.E.; Hollander, R.W.; Pijpelink, J. Temperature Dependence of BaF_2 Scintillation Light Yield. *Nucl. Instrum. Methods Phys. Res. A* **1985**, *238*, 564–565. [CrossRef]
30. Linardatos, D.; Konstantinidis, A.; Valais, I.; Ninos, K.; Kalyvas, N.; Bakas, A.; Kandarakis, I.; Fountos, G.; Michail, C. On the Optical Response of Tellurium Activated Zinc Selenide ZnSe:Te Single Crystal. *Crystals* **2020**, *10*, 961. [CrossRef]
31. Tseremoglou, S.; Ntoupis, V.; Linardatos, D.; Valais, I.; Michail, C.; Bakas, A.; Ninos, K.; Lavdas, E.; Kandarakis, I.; Fountos, G.; et al. Temperature Dependence of the Luminescence Output of $LaCl_3$:Ce Single Crystal Scintillator. *Procedia Struct. Integr.* **2023**, *47*, 119–124. [CrossRef]
32. Morelli, D.T.; Heremans, J. Thermal Conductivity of Single-crystal Barium Fluoride. *J. Appl. Phys.* **1988**, *63*, 573–574. [CrossRef]
33. Jiang, H.; Rooh, G.; Kim, H.J.; Lee, J.M.; Lee, Y.J.; Kim, S. Study on Scintillation Characteristics of BGSO Single Crystals. *IEEE Trans. Nucl. Sci.* **2014**, *61*, 323–327. [CrossRef]

Disclaimer/Publisher's Note: The statements, opinions and data contained in all publications are solely those of the individual author(s) and contributor(s) and not of MDPI and/or the editor(s). MDPI and/or the editor(s) disclaim responsibility for any injury to people or property resulting from any ideas, methods, instructions or products referred to in the content.